

The highly processive kinesin-8, Kip3, switches microtubule protofilaments with a bias towards the left

Volker Bormuth,^{†‡} Bert Nitzsche,^{†§} Felix Ruhnau,^{†§} Aniruddha Mitra,^{†§} Marko Storch,[†]
Burkhard Rammner,[¶] Jonathon Howard,[†] and Stefan Diez^{†§}

[†]Max Planck Institut of Molecular Cell Biology and Genetics, Pfotenhauerstrasse 108, 01307 Dresden, Germany; [‡]Current address: Institut Curie, UMR168, 26, Rue d'Ulm, 75005 Paris, France; [§]B CUBE – Center for Molecular Bioengineering, Technische Universität Dresden, Arnoldstrasse 18, 01307 Dresden, Germany; [¶]Scimotion, Beerenweg 8, 22761 Hamburg, Germany

1. Experimental details

Microtubules featuring >95% 14 protofilaments were assembled as described previously (1). A mixture of bovine tubulin containing 1% rhodamine-labelled and 1% biotinylated tubulin was incubated for 2 h at 37°C in BRB80 (80 mM Pipes (Sigma), pH 6.9, with KOH (VWR), 1 mM EGTA (Sigma), 1 mM MgCl₂ (VWR)), 1 mM GMP-CPP (Jena Bioscience), 4 mM MgCl₂. The assembled microtubules were sedimented by centrifugation in a Beckman Airfuge at 100,000 g for 5 min. The pellet was resuspended in BRB80 augmented with 10 mM taxol. Kip3 was expressed in Sf9 cells and purified as described previously (2).

Gliding motility assays and FLIC microscopy were performed similar as described previously (1). A flow chamber was constructed from (i) a 10 mm x 10 mm silicon chip with a transparent oxide layer of about 30 nm coated with dichlorodimethylsilane (Sigma Aldrich), (ii) a 22 mm x 22 mm coverslip passivated with a PEG layer and (iii) NESCO film as a spacer. Thereby formed flow channels were 10 mm x 1.5 mm x 100 µm in dimension.

The following solutions were perfused into the flow channel consecutively: (i) Fab fragments (anti-mouse IgG [Fc specific], Sigma-Aldrich; varying concentrations between 1.3 µg/ml and 20 µg/ml), (ii) PBS to wash out residual Fab fragments, (iii) Pluronic F127 (Sigma, P2443, 1% in PBS and 0.2-µm filtered) to block the surface against unspecific protein adsorption (15 min incubation), (iv) PBS to wash out residual Pluronic F127 (Sigma-Aldrich), (v) PBS augmented with 0.5 mg/ml anti GFP monoclonal antibodies (mouse, clone 106A20 produced in-house by MPI-CBG antibody facility) and 0.4 mg/ml casein, (vi) BRB80 to wash out residual GFP antibodies, (vii) motor dilution buffer (BRB80 augmented with 112.5 mM KCl, 1 mM ATP, 0.2 mg/ml casein, 10 mM DTT, 0.1% Tween20 [Sigma-Aldrich]), (viii) 20 µg/ml Kip3 in motor dilution buffer, (ix) motor dilution buffer to wash out residual Kip3, (x) Imaging solution (motor dilution buffer augmented with 40 mM D-glucose, 110 µg/ml glucose oxidase, 22 µg/ml catalase) augmented with microtubules and 100 pM Qdot 655 streptavidin conjugate (Invitrogen), (xi) imaging solution to wash out residual microtubules and QDs.

To ensure that the short pitches of the rotations observed in our experiments were a robust finding, we repeated the experiments over a wide range of motor densities. These measurements included experiments at very low motor densities, close to conditions where microtubules were propelled by single motors. While we did notice a wider spread in the data at low motor density, we did not observe any microtubules rotating with pitches larger than a fourth of the microtubule supertwist. We therefore conclude that Kip3 switches between protofilaments instead of tracking them reliably.

2. Imaging and data evaluation

Sequential imaging of QDs and microtubules was performed similarly as described previously (1). Differently, for imaging of QDs we used the 488 nm line of an argon/krypton ion laser (Coherent Innova 70C Spectra) as excitation light source in combination with appropriate filters: exc 475/42, em 655/40, dc 517 LP (all Semrock). Control images of microtubules were recorded using a Lumen 200 metal halide lamp (Prior Scientific Instruments) combined with appropriate filters: exc 535/50, em 610/75, dc 565 LP (all Chroma).

FLIC intensities and *xy*-coordinates of QDs as functions of the distance traveled by the respective microtubules were determined using inhouse-developed tracking software FIESTA (1,3). The paths of microtubules were estimated by moving averages of the tracked QD positions.

3. Determination of the kinesin-8 neck linker length

To determine the neck linker length of Kip3, we analyzed a collection of kinesin-8 from human, mouse, yeast and zebra fish. We compared a stretch of 70 amino acids starting with the RA motif from helix six at the end of the motor domain. We found that the next amino acid lysine is conserved in the analyzed kinesin-8 group and we assume this residue to be the start of the neck linker in agreement with other kinesins (4). Using PCOILS we predicted the start of the coiled coil region within the same set of kinesin-8s to be aa453 (V453 for Kip3; Fig. S1), which is conserved according to a sequence alignment with ClustalW. Thus the neck linker of kinesin-8s is 17 amino acids long and in the case of Kip3 spans the region from **K436** to **H452**: **KEIKTKIIRNQQLSRH** (Fig. S2).

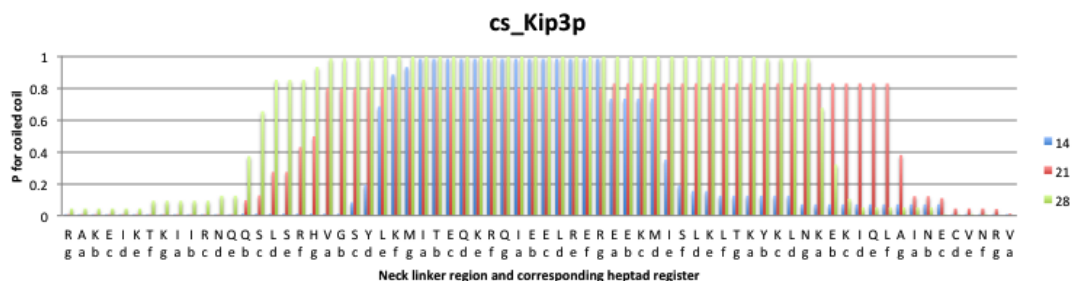


FIGURE S1 Results of PCOILS analysis of the 70 amino acids stretch starting at R434. Probability scores are plotted over the peptide position with the most likely register for a coiled coil heptad. The probability was calculated based on three different window sizes: 14 (blue), 21 (red) and 28 (green).

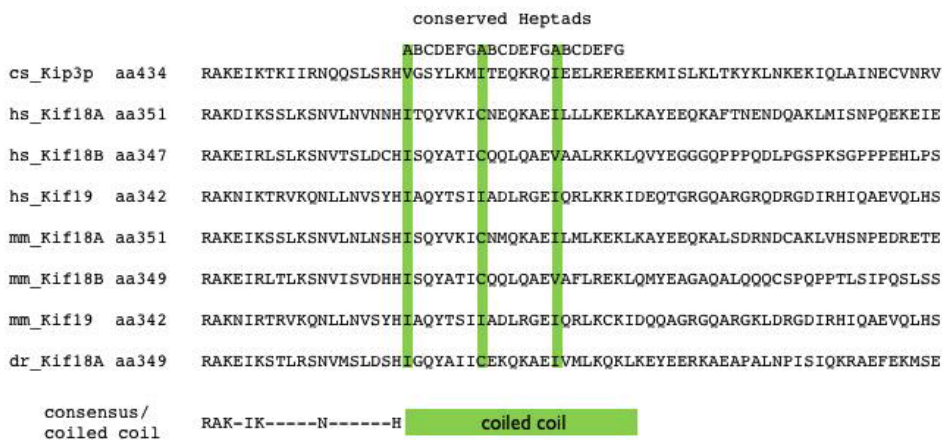


FIGURE S2 The predicted start of the coiled coil is well conserved in the kinesin-8 family. All kinesin-8 analyzed have a 17 amino acid long neck linker with five conserved residues.

4. Modeling

Scimotion developed custom-written C++ routines for the 3D-animation software Maya (Autodesk) to model and animate proteins with atomic coordinates from x-ray structures and electron tomography. Using this tool we reconstructed a microtubule based on the atomic coordinates of microtubule sections (kindly provided by Kenneth Downing) and modeled a Kip3 molecule (based on the atomic coordinates for kinesin-1 where additional amino acids in the Kip3 motor domain compared to kinesin-1 were inserted as unstructured peptide chains) on this microtubule in five steps. First, we folded the sequence of the rear-head motor domain in its ATP state and oriented it relative to the microtubule with the structural data available for the homologous kinesin-1 KIF1a crystallized with the ATP analogue AMP-PNP (pdb code 2HXF) (5). Second, we folded the front head in its ADP state according to the KIF1a-ADP structure (pdb ID 2HXF) (5). Third, we docked the neck linker of the rear head from amino acid K436 to Q447 according to the structural data of the kinesin-1 KHC neck linker (K325 to E336) (6) and left the neck linker of the front head undocked.

For the undocked neck linker regions dihedral angles were selected that are compatible with the Ramachandran plot. Fourth, the sequence following the neck linker region was modeled as a coiled coil dimerization domain starting at V453. Fifth, the additional amino acids in the Kip3 motor domain (M1 to A435) compared to kinesin-1 were modeled as unstructured random coils and placed such to minimize their interaction with the neck linker. For the visualization of the different binding configurations in Fig. 2 B we artificially unfolded the first heptad repeat of the coiled coil region.

Our modeling can also be used to make predictions for the rotations induced by motors whose neck linkers have been extended or truncated. However, the corresponding experiments are difficult; for example, internally consistent effects of changing neck linker length on processivity have only been obtained when the context of the amino-acid changes has been carefully controlled (7,8).

5. Estimation of the maximal distance the free neck linkers can span

The following elements contribute to the total maximum free neck linker length (from the first undocked amino acid of the rear head neck linker (S448) to the first amino acid of the front head neck linker (K436)):

- **rear head:** 5 aa (S448-V452 undocked)
- **front head:** 17 aa (K436-V452 undocked)
- **start of coiled coil:** 3.6 Å which is the estimated distance between the two C_α-atoms at the beginning of the neck helix where the neck linkers of front and rear head meet

The length of an amino acid is estimated to be 3.7 Å. This is the upper limit with maximally stretched dihedral angles that are still compatible for all amino acids according to the Ramachandran plot and with standard bond length and angles (following table).

bond length	dihedral angle	bond angle
1.33 Å (C-N)	180° (w)	123° (C _α -N-C)
1.53 Å (C-C _α)	180° (ψ)	114° (N-C-C _α)
1.46 Å (N-C _α)	180° (φ)	120° (C-C _α -N)

The maximal distances the free neck linker parts can span then add up to:

$$\text{Kip3: } L = (5 + 17) \text{ aa} * 3.7 \text{ Å/aa} + 3.6 \text{ Å} = 85.0 \text{ Å}$$

$$\text{Kinesin-1: } L = (2 + 14) \text{ aa} * 3.7 \text{ Å/aa} + 3.6 \text{ Å} = 62.8 \text{ Å}$$

6. Distance measurements given in Fig. 2 C of main text

tubulin-tubulin: Distance (as determined from the length of a non-uniform rational basis spline [NURBS] curve with degree 1) between the H406 amino acids of two adjacent alpha tubulins.

3D model: Minimal length of a “rope” from the first undocked amino acid of the rear head neck linker (S448, the “start point”) to the first amino acid of the front head neck linker (K436, the “end point”) respecting the volume excluded by the Kip3 molecule itself. The optimal path of the rope was determined manually in the 3D software by the following procedure: A first NURBS curve (with degree 1) just connecting the start and end point was built. It served as a directional guide for the second curve. A second NURBS curve (with degree 3) connecting the start and end point partly via several intermediate points was constructed. The minimal allowed distance between atoms of the neck linker and the surface of the motor domains was always set to 4.8 Å, which is the distance of two opposing C_α-atoms in an anti-parallel beta sheet. To determine the *distance to the right and front-right* the second NURBS curve reached from the start point in a straight line to the top back of the front head and then followed the shape of the front head to the end point. To determine the *distance to the front and front-left* the second NURBS curve reached in a straight line directly from the start to the end point. To determine the *distance to the left* the second NURBS curve first reached around the front end of the rear head (towards the left) and then continued in a straight line to the end point.

7. Acknowledgements

We thank K. Downing for kindly providing PDB files of microtubule sections, C. Bräuer for technical assistance, G. Fink and E. Schäffer for comments on the manuscript, as well as F. Friedrich for help on the graphics. This work was supported by the ERC (starting grant 242933), the DFG (Heisenberg program, S.D.), the FEBS society (fellowship, V.B.) and the Max-Planck-Society.

8. Supporting References

1. Nitzsche, B., F. Ruhnnow, and S. Diez. 2008. Quantum-dot-assisted characterization of microtubule rotations during cargo transport. *Nat. Nanotechnol.* 3:552-556.
2. Varga, V., J. Helenius, K. Tanaka, A. A. Hyman, T. U. Tanaka, and J. Howard. 2006. Yeast kinesin-8 depolymerizes microtubules in a length-dependent manner. *Nat. Cell Biol.* 8:957-960.
3. Ruhnnow, F., D. Zwicker, and S. Diez. 2011. Tracking Single Particles and Elongated Filaments with Nanometer Precision. *Biophys. J.* 100:2820-2828.
4. Hariharan, V. and W. O. Hancock. 2009. Insights into the Mechanical Properties of the Kinesin Neck Linker Domain from Sequence Analysis and Molecular Dynamics Simulations. *Cell. Mol. Bioeng.* 2:177-189.
5. Kikkawa, M. and N. Hirokawa. 2006. High-resolution cryo-EM maps show the nucleotide binding pocket of KIF1A in open and closed conformations. *EMBO J.* 25:4187-4194.
6. Kozielski, F., S. Sack, A. Marx, M. Thormahlen, E. Schonbrunn, V. Biou, A. Thompson, E. M. Mandelkow, and E. Mandelkow. 1997. The crystal structure of dimeric kinesin and implications for microtubule-dependent motility. *Cell.* 91:985-994.
7. Yildiz, A., M. Tomishige, A. Gennerich, and R. D. Vale. 2008. Intramolecular strain coordinates kinesin stepping behavior along microtubules. *Cell.* 134:1030-1041.
8. Shastry, S. and W. O. Hancock. 2010. Neck linker length determines the degree of processivity in kinesin-1 and kinesin-2 motors. *Curr. Biol.* 20:939-943.